Joint and iterative detection and decoding of differentially encoded COFDM systems

Wim J. van Houtum
Catena Radio Design
Son en Breugel, The Netherlands
Technische Universiteit Eindhoven
Eindhoven, The Netherlands

Frans M. J. Willems
Technische Universiteit Eindhoven
Eindhoven, The Netherlands

***Abstract*—Divsalar and Simon showed that with multi-symbol differential detection, the performance gap between two-symbol differential detection and coherent detection of differentially encoded phase shift keying can be closed.**

To close this gap for single-carrier differentially encoded phase shift keying with interleaving and convolutional encoding, Peleg et al. proposed a joint and iterative multi-symbol detection and decoding scheme that regards the differential encoding as inner component code of a serially concatenated code.

Several data-, audio- and video-broadcast systems are differentially encoded multi-carrier systems and use time multiplexing of the transmitted services to reduce receiver complexity. The commonly used receiver-structure for these systems does not perform joint and iterative multi-symbol detection and decoding.

The present work extends the use of the single-carrier iterative decoding scheme proposed by Peleg et al. to demodulate differentially encoded multi-carrier systems. A novel two-dimensional block-based demodulation is proposed that maintains both the multi-symbol differential detection coding gain and the reduction in receiver complexity by time-multiplexing.

Simulations show that with comparable receiver-complexity, the proposed multi-carrier scheme outperforms the single-carrier scheme by ≈ 0.9 dB. Furthermore, the receiver complexity can be reduced up to a factor of four and a half compared to the single-carrier scheme. Finally, the proposed multi-carrier scheme outperforms "classical" two-symbol differential detection with soft-decision Viterbi-decoding by ≈ 2.8 dB with one iteration and by ≈ 1.2 dB without iterations.

I. Introduction

Differential Encoding (DE) enables receivers to perform non-coherent detection. These non-coherent detection receivers become more robust against ambiguities and impairments of the phase of the received signal compared to coherent detection receivers. However, there is a "performance gap" between differential detection and coherent detection of differentially encoded multi-phase shift keying (DE-MPSK) [1].

For the additive white Gaussian noise (AWGN) channel with a time-invariant (unknown) phase, Divsalar and Simon [1] showed that if the observation interval is chosen to be sufficiently long i.e. Multi-Symbol Differential Detection (MSDD), the performance gap between the "conventional" two-symbol differential detection (2SDD) and coherent detection of DE-MPSK can be closed. They propose to make use of maximum-likelihood sequence estimation (MLSE) of the transmitted phases rather than symbol-by-symbol detection as in conventional differential detection [1]. In the rest of this paper we will refer to the improvement by expansion of the observation interval as: "*MSDD coding gain*".

Peleg and Shamai [2] proposed an iterative decoding scheme that regards the DE as inner component code of a serially concatenated code and the convolutional encoding as outer component code. The Soft-input Soft-output (SiSo) a-posteriori probability inner-decoder and SiSo a-posteriori probability outer-decoder improve their decision values by reliability information coming from the outer-decoder, respectively, the inner-decoder as proposed by Benedetto et al. [3] and ten Brink et al. [4], where the inner-decoder is replaced by a soft-demapper. The serial concatenation of MSDD and soft-decision convolutional decoding with reliability information exchange yields a significant improvement and we will refer to this improvement as: "*MSDD iterative coding gain*" [2]. However, a serious drawback of the iterative decoding scheme proposed by Peleg and Shamai in [2] is that the computational complexity of the inner-decoder increases exponentially by the number of symbols in the observation interval and linearly with the number of iterations.

To overcome the exponential complexity of the inner-decoder and maintain the MSDD iterative coding gain, Peleg et al. [5] proposed a trellis-based inner-decoder. They proposed to discretize the phase of the desired signal into several equispaced values and calculated the a-posteriori probability of the differentially encoded information phases using the BCJR-algorithm described by Bahl et al. [6]. In the rest of this paper, we will refer to the trellis-based inner-decoder proposed by Peleg et al. [5] as: "*the single-carrier Peleg-trellis inner-decoder*".

The digital audio broadcast (DAB), DAB+ and Terrestrial-Digital Multimedia Broadcasting (T-DMB) systems use Multi-carrier modulation (MCM). The principle of MCM in the DAB-family is based upon orthogonal frequency division multiplexing (OFDM), where each OFDM-subcarrier is modulated by $\frac{\pi}{4}$-DE-Quaternary PSK [7]. The DAB-family uses time multiplexing of the transmitted services to enable receivers to process only those OFDM-symbols that contain the data of the selected/required services [7]. With this, "*per service symbol processing*", the receiver complexity i.e. the number of

978-1-4244-5247-7/09/$26.00 ©2009 IEEE

OFDM-symbols that need to be processed, can be significantly reduced. For example, frequently used DAB audio-services in transmission mode-I only need up to four out of eighteen OFDM symbols [7], which results in a receiver complexity reduction of a factor of four and a half.

The classical multi-carrier receiver-structure for the DE-COFDM DAB-services is based on Differential QPSK (DQPSK) i.e. 2SDD of DE-QPSK, Viterbi decoding with soft-decisions and no MSDD or iterative decoding [8]. In addition, the studies [1] − [4] have emphasized single-carrier iterative decoding for QPSK or Binary-PSK (BPSK) and no attention has been paid to iterative decoding for multi-carrier DE-QPSK or multi-carrier DE-BPSK. It would be of interest to investigate the possibility, complexity and performance of applying iterative decoding with, for example, the single-carrier Peleg-trellis inner-decoder to the per service symbol processing of the DAB-family broadcast systems and more in general to DE-COFDM systems.

The present work extends the use of the single-carrier Peleg-trellis inner-decoder to demodulate the multi-carrier DE modulation code of differentially encoded COFDM systems. A novel two-dimensional (2D)-block-based demodulation of the multi-carrier DE modulation code is proposed to maintain both the MSDD iterative coding gain [5] and the reduction in receiver complexity by per service symbol processing [7]. With the proposed 2D-block-based demodulation the length of the trellis is equal to the size of the 2D-block, which is the product of multiple OFDM-symbols and multiple OFDM-subcarriers. The extension of the trellis-length by also taking the OFDM subcarriers into account enables per service symbol processing by almost no loss in MSDD iterative coding gain, as will be shown by simulations. In the rest of this paper, we will refer to this new 2D trellis-based inner-decoder as: "*the multi-carrier Peleg-trellis inner-decoder*".

The plan of this paper is as follows. Section II describes the single-carrier Peleg-trellis inner-decoder for multi-carrier DE-COFDM systems with the possibility of per service symbol processing. In Section III the DE-COFDM broadcast system model is constructed which is used to study the single-carrier Peleg Trellis inner-decoder. A novel extension of the single-carrier Peleg-trellis inner-decoder with 2D-block-based differential detection is proposed and tested by simulations in Section IV. Finally, Section V discusses the obtained simulation results for the newly proposed inner-decoder applied on a multi-carrier DE-COFDM system with the possibility of per service symbol processing.

II. The General Problem

The general problem of using the single-carrier Peleg-trellis inner-decoder for multi-carrier DE-COFDM systems with the possibility of per service symbol processing will be studied in this section.

MSDD per OFDM-subcarrier needs to be performed if the single-carrier Peleg-trellis inner-decoder is applied to multi-carrier DE-COFDM systems where DE-QPSK is performed between identical OFDM-subcarriers of two consecutive OFDM-symbols. Consequently, the length of the observation interval for MSDD is equal to the number of OFDM-symbols, which need to be processed. Due to the per service symbol processing, the length of the trellis is rather limited, for example up to four, and simulations show that there is a significant loss in MSDD (iterative) coding gain for such a short trellis. To overcome the loss in MSDD (iterative) coding gain the length of the trellis should be extended, this means, for the single-carrier Peleg-trellis inner-decoder, that more OFDM-symbols need to be processed and the receiver complexity will be increased. This is in contradiction with the possibility of per service symbol-processing, which was introduced for significantly decreasing the complexity of the receiver [7].

III. DE-COFDM broadcast systems

Terrestrial digital broadcasting systems like DAB, DAB+ and T-DMB comprises a combination of convolutional coding and $\frac{\pi}{4}$-DE-QPSK with OFDM and time multiplexing of the transmitted services to enable per service symbol processing [7]. The $\frac{\pi}{4}$-DE-QPSK is performed between identically positioned, within an OFDM-symbol, OFDM-subcarriers of two consecutive OFDM-symbols. In the sequel of this paper we will use these DE-COFDM broadcast systems as our proposed system for iterative decoding of the differentially encoded received QPSK-signal.

A. Model of DE-COFDM transmission over an AWGN channel

A convolutional encoder encodes sequences of N_b information bits to sequences of N_c coded bits. The convolutional encoder has a code-rate $R_c = \frac{1}{4}$, a constraint length of $K = 7$ and generator polynomials $\{g_0 = 133, g_1 = 171, g_2 = 145, g_3 = 133\}$. In addition, higher code-rates are obtained via puncturing of the mother code i.e. rate-compatible punctured convolutional codes (RCPC codes) [9]. We use, conform [5], the de-facto industry standard $R_c = \frac{1}{2}$ convolutional code with generator polynomials $g_0 = 133$ and $g_1 = 171$, which is equal to the punctured convolutional code represented by puncturing vector $PI = 8$ of Table 34 in [7].

The DAB, DAB+ and T-DMB bit-reversal time interleaver and block frequency interleaver are modeled by a bit-wise uniform block interleaver generated for each simulated code block of bits x_i resulting in a sequence of bits x_j. Thus any permutation of the N_c coded bits is a permissible interleaver and is selected with equal probability conform [5].

An QPSK mapper maps, with Gray encoding, a bit pair $(x^1_{l,k}, x^2_{l,k})$ to an QPSK symbol; $q_{l,k} = \exp(j\Delta\phi_{l,k})$ with $\Delta\phi_{l,k} \in \{\frac{\pi}{4}, \frac{3\pi}{4}, \frac{5\pi}{4}, \frac{7\pi}{4}\}$.

A modulator performs differential encoding between symbols $s_{l-1,k} = \exp(j\phi_{l-1,k})$ and $s_{l,k} = \exp(j\phi_{l,k})$;

$$s_{l,k} = s_{l-1,k} \cdot q_{l,k} \quad (1)$$

$$\phi_{l,k} = \phi_{l-1,k} + \Delta\phi_{l,k} \quad (2)$$

with $\phi_{l,k} \in \{0, \frac{\pi}{2}, \pi, \frac{3\pi}{2}\}$ or $\phi_{l,k} \in \{\frac{\pi}{4}, \frac{3\pi}{4}, \frac{5\pi}{4}, \frac{7\pi}{4}\}$ for $k = [-\frac{K}{2}, \ldots, -1, 1, \ldots, \frac{K}{2}]$, $l = [0, 2, 4, \ldots, L-2]$, respectively,

$l = [1, 3, 5, \ldots, L-1]$ and where L and K are defined as the *Frame-length* respectively the *Frame-width*. In addition, the K initial $\frac{\pi}{4}$-DE-QPSK symbols $\{s_{0,k}\}$ are defined in [7].

DE-QPSK symbol $s_{l-1,k}$ modulates an OFDM subcarrier at frequency bin $f_k = k \cdot \Delta f = k \cdot \frac{1}{T_u}$ with T_u is the inverse of the subcarrier spacing, and DE-QPSK symbol $s_{l,k}$ modulates a subcarrier at the same frequency bin f_k of the consecutive OFDM symbol. Without loss of generality we assume that $f_{k=0}$ is not used for data transmission [7].

The transmitted complex baseband signal per frame of L OFDM-symbols each with K modulated subcarriers can now be given by;

$$\begin{aligned} s(t) &= \sum_{l=0}^{L-1} \sum_{\substack{k=-\frac{K}{2} \\ k \neq 0}}^{\frac{K}{2}} s_{l,k} e^{j2\pi f_k (t - lT_s)} \cdot w(t - lT_s) \\ & -T_g \leq t < LT_s - T_g \end{aligned} \tag{3}$$

with the rectangular window function $w(\tau)$ for each OFDM symbol is defined as;

$$w(\tau) = \begin{cases} 1 & \text{for } -T_g \leq \tau < T_u \\ 0 & \text{otherwise} \end{cases} \tag{4}$$

and $T_s = T_g + T_u$ is the duration of one OFDM symbol with T_g the duration of the guard-interval.

The OFDM part at the receiver performs match-filtering on each OFDM subcarrier with a rectangular filter impulse response of duration T_u resulting in

$$\begin{aligned} r_{l,k} &= \frac{1}{T_u} \int_{t=lT_s}^{lT_s+T_u} r(t) e^{-j2\pi f_k (t - lTs)} dt \\ &= s_{l,k} e^{j\theta_{l,k}} + \eta_{l,k} \end{aligned} \tag{5}$$

where $\eta_{l,k}$ represents a complex AWGN sample with variance σ_η^2 at subcarrier k of OFDM symbol l and $\theta_{l,k}$ is an arbitrary phase introduced by the channel which is assumed to be uniformly distributed in the interval $(-\pi, \pi]$. In addition, the transmission-channel is assumed to be an AWGN channel where $\theta_{l,k}$ is independent of l and k during a frame i.e. for each frame $\theta_{l,k} = \theta$, now analogous to (5), the received DE-QPSK symbols $r_{l,k}$ for each frame are expressed as;

$$\mathbf{r} = \mathbf{s} e^{j\theta} + \mathbf{n} \tag{6}$$

where $\mathbf{r}$, $\mathbf{s}$ and $\mathbf{n}$ are the frame-sequences of $r_{l,k}$, $s_{l,k}$ and $\eta_{l,k}$, respectively. For clarity and brevity we will focus on the AWGN-channel, however, the multi-carrier Peleg-trellis inner-decoder is not limited to the AWGN-channel if sufficient channel state information is available and an appropriate size of the 2D-block is chosen. This will be addressed by the authors in a forthcoming paper.

B. 2SDD and Viterbi decoding

A commonly used receiver-structure consists of classical 2SDD on each OFDM subcarrier to obtain an estimate of a QPSK symbol at frequency bin f_k [8]

$$\hat{q}_{l,k} = r_{l,k} \cdot r_{l-1,k}^*. \tag{7}$$

The convolutional decoding in a commonly used receiver is performed by maximum Likelihood sequence estimation (MLSE) with the "well-known" Viterbi algorithm, which uses as soft decisions, from the demodulator, the real and imaginary parts of $\hat{q}_{l,k}$ [9]

$$\begin{aligned} \lambda_{l,k}^1 &= \Re\{\hat{q}_{l,k}\} \\ \lambda_{l,k}^2 &= \Im\{\hat{q}_{l,k}\} \end{aligned} \tag{8}$$

where $\lambda_{l,k}^i$ represents the soft decision information of the received coded bit $\hat{x}_{l,k}^i$ with $i \in \{1, 2\}$ and $\Re(\cdot)$, respectively, $\Im(\cdot)$ denoting the real and imaginary part of a complex number.

C. Exhaustive search MSDD and Viterbi decoding

Divsalar and Simon showed in [1] that MSDD fills the gap between classical 2SDD and coherent detection for DE-MPSK. They derived the a-posteriori probability (APP) for N-length sequences of received differentially encoded symbols on the AWGN channel with an uniformly distributed unknown channel phase. They showed that MLSE of the N-length sequences will, for $N = \infty$, achieve the performance of coherent detection for DE-MPSK. Moreover, they showed that increasing the observation interval with only one or two symbols already gives a significant improvement for uncoded MPSK i.e. ≈ 1.5 dB at a bit error probability (BER) of $1 \cdot 10^{-4}$ for uncoded DE-QPSK [1].

In addition, Divsalar et al. showed in [10] that the use of MSDD in a coded case, as it was true for the uncoded case, can also offer an improvement in error probability performance over conventional 2SDD. For example, an increase in the length of the observation interval with one symbol for two-state rate $1/2$ trellis-coded QPSK shows an MSDD coding gain in the order of ≈ 0.25 dB at a BER $1 \cdot 10^{-4}$ [10].

However, Divsalar et al. in [10] and others, referred to in [2], use MSDD methods that utilize the power of the error correcting codes and are not directly applicable to interleaved systems [2]. Peleg and Shamai addressed in [2], with their joint and iterative demodulation and decoding procedure, MSDD of DE-MPSK for interleaved systems. This iterative decoding scheme is based on the exchange of reliability information between the MSDD demodulator and a Soft-input Soft-output (SiSo) module, described by Benedetto in [3] using the efficient Bahl algorithm [6], as convolutional SiSo decoder. In the sequel of this paper we refer to this convolutional SiSo decoder as: "*the BCJR decoder*". In [2] the MSDD coding gain is equal to the improvement between 2SDD and MSDD at the first path through iterative decoding i.e. no iterations are performed. When no iterations are performed, the maximum likelihood decision statistic based on an observation interval of N successive MPSK symbols i.e. the soft-decision information, from the MSDD demodulator, for the convolutional decoding is given by Eqn. 1 of [2] with equal a-priori probabilities:

$$\Lambda_j = \sum_{C \in \mathbf{C}_j} P(\mathbf{R}|C) \tag{9}$$

where $\mathbf{C}_j$ are all modulation codewords corresponding to the sequences of bits $[x_1, \ldots, x_{N\log_2(M)}]$ having $x_j = 1$. According to [2], the conditional probability $P(\mathbf{R}|C)$ is given by Eqn. 9 in [1]

$$\begin{aligned} p(\mathbf{r}|\mathbf{s}) &= \int_{-\pi}^{\pi} p(\mathbf{r}|\mathbf{s},\theta)p(\theta)d\theta \\ &\sim I_0\left(\frac{2}{\sigma_\eta^2}\left|\sum_{n=1}^{N} r_n \cdot s_n^*\right|\right), \end{aligned} \tag{10}$$

where I_0 is the zero-th order modified Bessel function and n is a function of l and k. The approximation in (10) is obtained, by removing the common terms to all codewords, they are irrelevant to the decoding process [2]. Now, the soft decision information for the received coded bit pair $(\hat{x}_{l,k}^1, \hat{x}_{l,k}^2)$, representing QPSK symbol $\hat{q}_{l,k}$, can be computed by substitution of (10) into (9), which yields

$$\lambda_{l,k}^i = \sum_{C\in\mathbf{C}_j} I_0\left(\frac{2}{\sigma_\eta^2}\left|\sum_{n=1}^{N} r_n \cdot s_n^*\right|\right) \tag{11}$$

where $i \in \{1,2\}$ and j is a function of l and k.

Simulation results without iterations in [2] reveal for DE-QPSK with an observation interval extension by three symbols $(N = 5)$ that the MSDD coding gain is ≈ 0.3 dB at a BER $1 \cdot 10^{-4}$ and is still ≈ 2.5 dB away from closing the gap with coherent detection of DE-QPSK and convolutional decoding.

Since, the MSDD coding gain is obtained without iterations the soft-output information of the BCJR outer-decoder is not required and the output can be a two-level "hard-decision" output obtained via, for example, the Viterbi algorithm. Simulations, indeed, show similar results for the MSDD coding gain by either using as outer decoder; the Viterbi algorithm or the BCJR algorithm without iterations and "two-level clipping". The MSDD coding gain is obtained by an exhaustive search on M^N possible sequences of length N. In the rest of this paper we wil refer to this MSDD demodulator proposed by Peleg and Shamai in [2] as: "*the exhaustive search MSDD demodulator*".

D. Single-carrier trellis-based MSDD and Viterbi decoding

To avoid the exponential complexity of the exhaustive search MSDD demodulator, Peleg et al. in [5] proposed to replace the exhaustive search MSDD demodulator by a trellis-based MSDD demodulator i.e. the single-carrier Peleg-trellis inner-decoder.

Using the single-carrier Peleg-trellis inner-decoder, the phase of each DE-QPSK symbol is discretised into Q equi-spaced values and these equispaced values represent the Q states of the trellis. In addition, it is assumed that the discrete phases of the DE-QPSK symbols represent a Markov process [5]. Let $\mathbf{r}_{k_1}$, $\boldsymbol{\psi}_{k_1}$, $\boldsymbol{\phi}_{k_1}$, $\boldsymbol{\Delta\psi}_{k_1}$ and $\boldsymbol{\Delta\phi}_{k_1}$ be the sequences at frequency bin $f_{k=k_1}$ of r_{l,k_1}, ψ_{l,k_1}, ϕ_{l,k_1}, $\Delta\psi_{l,k_1}$ and $\Delta\phi_{l,k_1}$, respectively. Now a path η_{k_1}, of length L, through the trellis is uniquely determined by the discretely distributed phases $\boldsymbol{\psi}_{k_1} = \boldsymbol{\phi}_{k_1} + \theta$ of the L DE-QPSK symbols, thus,

$$\begin{aligned} \Pr\{\mathbf{r}_{k_1}, \eta_{k_1}\} &= \Pr\{\mathbf{r}_{k_1}, \boldsymbol{\psi}_{k_1}\} \\ &= \Pr\{\boldsymbol{\psi}_{k_1}\}\Pr\{\mathbf{r}_{k_1}|\boldsymbol{\psi}_{k_1}\} \\ &= \Pr\{\boldsymbol{\psi}_{k_1}\}\left[\prod_{l=0}^{L-1}\Pr\{r_{l,k_1}|\psi_{l,k_1}\}\right] \end{aligned} \tag{12}$$

where the third equality is based on the assumption that the channel is memoryless [5].

The mapping of $\boldsymbol{\Delta\phi}_{k_1}$ to $\boldsymbol{\Delta\psi}_{k_1}$ is one to one, this implies

$$\Pr\left\{\boldsymbol{\Delta\psi}_{k_1}\right\} = \Pr\left\{\boldsymbol{\Delta\phi}_{k_1}\right\} \tag{13}$$

and since $\boldsymbol{\psi}_{k_1}$ is a one to one function of the arbitrary channel phase $\psi_{0,k_1} = \phi_{0,k_1} + \theta$ distributed uniformly over Q and of $\boldsymbol{\Delta\psi}_{k_1}$ we get

$$\Pr\left\{\boldsymbol{\psi}_{k_1}\right\} = \frac{1}{Q}\Pr\left\{\boldsymbol{\Delta\phi}_{k_1}\right\} = \frac{1}{Q}\prod_{l=1}^{L-1}\Pr\left\{\Delta\phi_{l,k_1}\right\}. \tag{14}$$

Combining Eqns. 12–14 yields:

$$\Pr\{\mathbf{r}_{k_1}, \eta_{k_1}\} = \frac{\Pr\{r_{0,k_1}|\psi_{0,k_1}\}}{Q}\prod_{l=1}^{L-1}\gamma_l(\eta_{k_1}) \tag{15}$$

$$\gamma_l(\eta_{k_1}) = \Pr\left\{\Delta\phi_{l,k_1}\right\}\Pr\{r_{l,k_1}|\psi_{l,k_1}\} \tag{16}$$

and with AWGN we have as DE-QPSK *symbol-metric*:

$$\Pr\{r_{l,k_1}|\psi_{l,k_1}\} = \frac{1}{\pi\sigma_\eta^2}e^{\frac{-\left|r_{l,k_1}-e^{j\psi_{l,k_1}}\right|^2}{\sigma_\eta^2}}, \tag{17}$$

this result is similar to Eqn. 10 in [5], where $2\sigma^2 = \sigma_\eta^2$ and i is a function of l and k_1. As was suggested in [5], the a-posteriori probabilities of the coded bits mapped to the QPSK-symbols can also here be evaluated by the efficient BCJR-algorithm described in [6]. We will, as in [5], only give the basic equations of the BCJR-algorithm for further reference.

The probability $\alpha_{l,k_1}(s)$ is calculated for state s at time l in the trellis by the forward recursion [6]:

$$\alpha_{l,k_1}(s) = \sum_{s'}\alpha_{l-1,k_1}(s')\gamma_{l,k_1}(s',s) \tag{18}$$

with $\alpha_{0,k_1}(s') = \frac{\Pr\{r_{0,k_1}|\psi_{0,k_1}=s'\}}{Q}$. The probability $\beta_{l,k_1}(s)$ is calculated for state s at time l in the trellis by the backward recursion [6]:

$$\beta_{l,k_1}(s) = \sum_{s''}\beta_{l+1,k_1}(s'')\gamma_{l+1,k_1}(s,s''). \tag{19}$$

with $\beta_{L-1,k_1}(s'') = 1, \forall s''$ and where $\alpha_{l,k_1}(s)$ and $\beta_{l,k_1}(s)$ represent the probabilities on state s of the k_1th subcarrier in the lth OFDM-symbol. In addition, $\gamma_{l,k_1}(s',s)$ represents the branch-probability related to connecting the state s' of the k_1th subcarrier in the $(l-1)$th OFDM-symbol with the state s of the k_1th subcarrier in the lth OFDM-symbol and is given by (16). The weight of a branch is calculated by [6]:

$$\sigma_{l,k_1}(s',s) = \alpha_{l-1,k_1}(s')\gamma_{l,k_1}(s',s)\beta_{l,k_1}(s). \tag{20}$$

The soft decision information for the received coded bit pair $(\hat{x}^1_{l,k_1}, \hat{x}^2_{l,k_1})$, representing QPSK symbol $\hat{q}_{l,k_1}$, can be computed by summing $\sigma_{l,k_1}(s',s)$ over a sub-set Λ^i_{l,k_1} of branches where $x^i_{l,k_1} = 1$ and normalizing by the sum of $\sigma_{l,k_1}(s',s)$ over all branches i.e. the complete set Λ_{l,k_1} at time l [5], which yields for the L-length sequences per subcarrier

$$\lambda^i_{l,k_1} = \frac{\sum_{\Lambda^i_{l,k_1}} \sigma_{l,k_1}(s',s)}{\sum_{\Lambda_{l,k_1}} \sigma_{l,k_1}(s',s)} \tag{21}$$

where $i \in \{1,2\}$. Hence, trellis-based MSDD with the single-carrier Peleg-trellis inner-decoder applied on a DE-COFDM frame m of size $S_m = L_m \times K_m$ will have a trellis length equal to the number of OFDM symbols L_m and is K_m times executed.

Divsalar et al. in [1] showed that the MSDD coding gain increases with increasing the length of the observation interval i.e. increasing the trellis length L_m of the single-carrier Peleg-trellis inner-decoder. Simulations are performed to determine the MSDD coding gain for different values of L_m. The simulation results will be discussed in Section V.

E. Joint and iterative single-carrier trellis-based MSDD and BCJR decoding

Peleg et al. showed in [5] that a large MSDD iterative coding gain can be achieved with joint and iterative trellis-based MSDD and convolution decoding.

As explained in [5], the BCJR outer-decoder yields estimates $\left\{\hat{b}_i\right\}$ of the information bits and extrinsic probabilities $\left\{\tilde{P}\left(x^i_{l,k}\right)\right\}$ of the coded bits.

The information $\lambda^i_{l,k}$ and $\tilde{P}\left(x^i_{l,k}\right)$, exchanged between the inner-decoder and outer-decoder, is decorrelated by the interleaver for proper iterative decoding [5]. In addition, as explained by Benedetto in [3] and also followed by Peleg et al. in [5], both; the 'intrinsic' part of the a-posteriori information coming from the inner decoder as the 'intrinsic' part of the a-posteriori information coming from the outer-decoder are removed.

The "extrinsic" probability pair $\left(\tilde{P}\left(x^1_{l,k_1}\right), \tilde{P}\left(x^2_{l,k_1}\right)\right)$ is fed back to the inner-decoder as the a-priori information $\Pr\{\Delta\phi_{l,k_1}\}$ of QPSK symbol $\hat{q}_{l,k_1}$ and the branch probability given by (16) can be rewritten as:

$$\begin{aligned} \gamma_l(\eta_{k_1}) &= \left[\prod_{i=1}^{\log_2(M)} \hat{P}\left(x^i_{l,k_1}\right)\right] \Pr\{r_{l,k_1}|\psi_{l,k_1}\} \\ &= \left[\tilde{P}\left(x^1_{l,k_1}\right)\tilde{P}\left(x^2_{l,k_1}\right)\right] \Pr\{r_{l,k_1}|\psi_{l,k_1}\} \end{aligned} \tag{22}$$

Simulations are performed to determine the MSDD iterative coding gain of joint and iterative L_m-length MSDD and SiSo convolutional decoding for DE-COFDM systems. The L_m-length MSDD is performed with the single-carrier Peleg-trellis inner-decoder and the convolutional decoding is performed with the BCJR outer-decoder. The simulations results, for different values of L_m and for a different number of iterations I, will be discussed in Section V.

IV. Joint and iterative detection and decoding of DE-COFDM broadcast systems

In this section the multi-carrier Peleg trellis inner-decoder, which is a novel extension of the single-carrier Peleg-trellis inner-decoder with 2D-block-based differential detection, is introduced for trellis-based MSDD in a DE-COFDM system. In addition, joint and iterative trellis-based MSDD with the multi-carrier Peleg-trellis and convolutional decoding with the BCJR outer-decoder for DE-COFDM systems is discussed.

A. Multi-carrier trellis-based MSDD and Viterbi decoding

As was explained in Section III-D, to improve the MSDD coding gain the L_m-length sequences need to be increased. This means, for MSDD with the single-carrier Peleg-trellis inner-decoder, that the receiver needs to process more OFDM-symbols and the complexity of the receiver will increase. In addition, the DAB, DAB+ and T-DMB broadcast systems use time multiplexing of the transmitted services or messages i.e. a transmission frame contains multiple DE-COFDM frames $\{m\}$, where each DE-COFDM frame m contains the data of a single message [7]. Consequently, only the L_m OFDM-symbols need to be processed, which contain the data of message m i.e. per service symbol processing. For a number of commonly used services of the DAB-family $L_m \leq 4$ i.e. per service symbol-processing only requires up to four OFDM-symbols to be processed by the receiver. Our simulation results, which will be discussed in Section V, reveal that for these small values of L_m the MSDD coding gain of the single-carrier Peleg-trellis inner-decoder is rather small.

As there are $S_m = L_m \times K_m$ DE-QPSK symbols available per DE-COFDM frame m and with $K_m \gg 1$, it is of interest to see if the S_m DE-QPSK symbols can be exploited to extend the length of the trellis from L_m to $S_m = L_m \times K_m$. The sequel of this section is devoted to show how to extend the trellis length from L_m to S_m and perform trellis-based MSDD by the multi-carrier Peleg-trellis inner-decoder on a DE-COFDM frame m.

The K_m initial DE-QPSK symbols $\{s_{0,k}\}$ for $l = 0$ are independently chosen from the same sets as the DE-QPSK symbols for $l \neq 0$. As $\boldsymbol{\psi}_k$ is a one to one function of $\phi_{0,k} + \theta$ and $\boldsymbol{\Delta\phi}_k$, the differential phases

$$\Delta\varphi_k = \begin{cases} \psi_{0,1} - \psi_{L_m-1,-1} = \phi_{0,1} - \phi_{L_m-1,-1}, \\ \qquad\qquad\qquad\qquad k = 1 \\ \psi_{0,k} - \psi_{L_m-1,k-1} = \phi_{0,k} - \phi_{L_m-1,k-1} \\ \qquad k = [-\frac{K}{2}+1, \ldots, -1, 2, \ldots, \frac{K}{2}], \end{cases} \tag{23}$$

are independent and belong to the same or a $\frac{\pi}{4}$ shifted set as the information phases $\{\Delta\phi_{l,k}\}$. Figure 1 shows this multi-carrier DE-QPSK frame-sequence for $L_m = 4$ in a graphical way where; the columns represent the OFDM-subcarriers, the rows the OFDM-symbols, the circles the DE-QPSK symbols and the arrows the path through the trellis. In addition, the upper part of (23) covers that subcarrier at $f_{k=0}$ is not used for data transmission, this can also be seen from Figure 1.

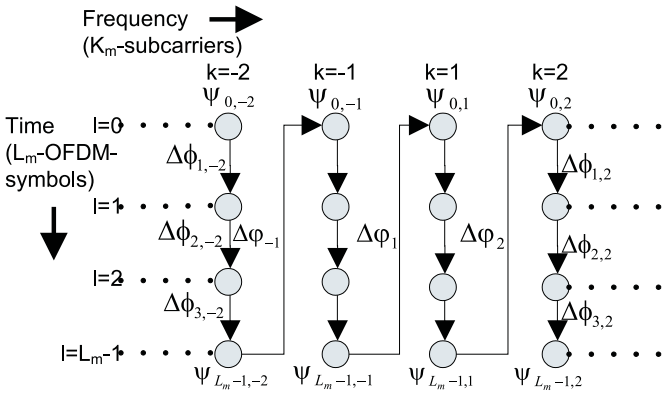

Fig. 1. Multi-carrier DE-QPSK frame-sequence for $S_m = 4 \times K_m$.

Now, also for the multi-carrier Peleg-trellis inner-decoder, it is assumed that the discrete phases $\{\psi_{l,k}\}$ represent a Markov process and a same approach will be followed as with the single-carrier Peleg-trellis inner-decoder explained in Section III-D. Let for a DE-COFDM frame m; $\mathbf{r}_m$ $\boldsymbol{\psi}_m$, $\boldsymbol{\phi}_m$, $\boldsymbol{\Delta\psi}_m$, $\boldsymbol{\Delta\phi}_m$ and $\boldsymbol{\Delta\varphi}_m$ be the frame-sequences of $r_{l,k}$, $\psi_{l,k}$, $\phi_{l,k}$, $\Delta\psi_{l,k}$, $\Delta\phi_{l,k}$, and $\Delta\varphi_k$, respectively. The path η_m, of length $S_m = L_m \times K_m$, through the trellis is uniquely determined by the discretely distributed phases $\boldsymbol{\psi}_m = \boldsymbol{\phi}_m + \theta$ of the S_m DE-QPSK symbols, thus,

$$\begin{aligned}\Pr\{\mathbf{r}_m, \eta_m\} &= \Pr\{\mathbf{r}_m, \boldsymbol{\psi}_m\} \\ &= \Pr\{\boldsymbol{\psi}_m\} \Pr\{\mathbf{r}_m | \boldsymbol{\psi}_m\} \\ &= \Pr\{\boldsymbol{\psi}_m\} \prod_{l=0}^{L_m-1} \prod_{\substack{k=-\frac{K_m}{2} \\ k\neq 0}}^{\frac{K_m}{2}} \Pr\{r_{l,k} | \psi_{l,k}\} \\ &= \Pr\{\boldsymbol{\psi}_m\} \left[\prod_{t=0}^{S_m-1} \Pr\{r_t | \psi_t\} \right] \end{aligned} \quad (24)$$

where the third equality is based on the assumption that the channel is memoryless and t, in the fourth equality, is a function of l and k.

The mapping of $\boldsymbol{\Delta\phi}_m$ and $\boldsymbol{\Delta\varphi}_m$ to $\boldsymbol{\Delta\psi}_m$ is one to one and $\boldsymbol{\Delta\phi}_m$ is independent of $\boldsymbol{\Delta\varphi}_m$, thus

$$\Pr\{\boldsymbol{\Delta\psi}_m\} = \Pr\{\boldsymbol{\Delta\phi}_m\} \Pr\{\boldsymbol{\Delta\varphi}_m\} \quad (25)$$

since $\boldsymbol{\psi}_m$ is a one to one function of the arbitrary channel phase $\psi_{0,0} = \phi_{0,0} + \theta$ distributed uniformly over Q and of $\boldsymbol{\Delta\psi}_m$ we get

$$\Pr\{\boldsymbol{\psi}_m\} = \frac{1}{Q} \Pr\{\boldsymbol{\Delta\phi}_m\} \Pr\{\boldsymbol{\Delta\varphi}_m\}. \quad (26)$$

Since a DE-COFDM frame m contains $(K_m(L_m-1) = (S_m - K_m))$ information phases $\{\Delta\phi_{l,k}\}$ and $K_m - 1$ differential phases $\{\Delta\varphi_k\}$

$$\Pr\{\boldsymbol{\psi}_m\} = \frac{1}{Q} \prod_{i=1}^{S_m-K_m} \Pr\{\Delta\phi_i\} \prod_{j=1}^{K_m-1} \Pr\{\Delta\varphi_j\}, \quad (27)$$

where i and j are functions of t.

Combining Eqns. 24–27 yields:

$$\Pr\{\mathbf{r}_m, \eta_m\} = \frac{\Pr\{r_0 | \psi_0\}}{Q} \prod_{t=1}^{S_m-1} \gamma_t(\eta_m) \quad (28)$$

with

$$\gamma_t(\eta_m) = \begin{cases} \Pr\{\Delta\varphi_t\} \Pr\{r_t | \psi_t\}, & t = nL_m \\ \Pr\{\Delta\phi_t\} \Pr\{r_t | \psi_t\}, & t \neq nL_m \end{cases} \quad (29)$$

where $n = \{1, 2, \ldots, K_m - 1\}$ and for the AWGN channel with the unknown channel phase the DE-QPSK symbol-metric becomes:

$$\Pr\{r_t | \psi_t\} = \frac{1}{\pi\sigma_\eta^2} e^{\frac{-|r_t - e^{j\psi_t}|^2}{\sigma_\eta^2}}. \quad (30)$$

Now, as was suggested for the Single-carrier Peleg-trellis inner-decoder, the a-posteriori probabilities of the coded bits mapped to the QPSK-symbols can also here be evaluated by the efficient BCJR-algorithm described in [6].

The probability $\alpha_t(s)$ is calculated for state s at time t in the trellis by the forward recursion with $\alpha_0(s') = \frac{\Pr\{r_0 | \psi_0 = s'\}}{Q}$, the probability $\beta_t(s)$ is calculated by the backward recursion with $\beta_{S_m-1}(s'') = 1, \forall s''$, the branch-probability $\gamma_t(s', s)$ is given by (29) and the weight of a branch is calculated by:

$$\sigma_t(s', s) = \begin{cases} \alpha_t(s') \Pr\{\Delta\varphi_t\} \Pr\{r_t | \psi_t = s\} \beta_t(s) \\ \qquad\qquad t = nL_m \\ \alpha_t(s') \Pr\{\Delta\phi_t\} \Pr\{r_t | \psi_t = s\} \beta_t(s). \\ \qquad\qquad t \neq nL_m \end{cases} \quad (31)$$

The "upper-part" of (31) are the $(K_m - 1)$ a-posteriori probabilities of the differential phases $\{\Delta\varphi_t\}$ and the "lower-part" of (31) are the $S_m - K_m$ a-posteriori probabilities of the information phases $\{\Delta\phi_t\}$. Since, the differential phases changes $\{\Delta\varphi_t\}$ do not contain information of the coded bit pairs $\{(x_t^1, x_t^2)\}$, representing QPSK symbols $\{q_t\}$, they need to be discarded for the deinterleaving and convolutional decoding proces i.e. they can not provide soft-decision information to the outer-decoder.

To calculate the soft decision information for the received coded bit pair $(\hat{x}_t^1, \hat{x}_t^2)$, representing received QPSK symbol $\hat{q}_t$, only the $S_m - K_m$ a-posteriori probabilities of the information phases $\{\Delta\phi_t\}$ given by the "lower-part" of (31) are summed over a sub-set Λ_t^i of branches where $x_t^i = 1$ and normalized by the sum of $\sigma_t(s', s)$ over all branches i.e. the complete set Λ_t at time t

$$\lambda_t^i = \frac{\sum_{\Lambda_t^i} \sigma_t(s', s)}{\sum_{\Lambda_t} \sigma_t(s', s)}, \quad (32)$$

which yields for the $S_m = L_m \times K_m$-length sequences;

$$\lambda_{l,k}^i = \frac{\sum_{\Lambda_{l,k}^i} \sigma_{l,k}(s', s)}{\sum_{\Lambda_{l,k}} \sigma_{l,k}(s', s)} \quad (33)$$

where $i \in \{1, 2\}$. Hence, trellis-based MSDD with the multi-carrier Peleg-trellis inner-decoder applied on a DE-COFDM

frame m of size $S_m = L_m \times K_m$ will have a trellis length equal to the number of OFDM symbols L_m times the number of subcarriers K_m i.e. *the multi-carrier Peleg-trellis inner-decoder performs 2D-trellis-based differential detection with the BCJR-algorithm*.

By increasing the length of the trellis i.e. the length of the observation interval to $S_m = L_m \times K_m$ the MSDD coding gain should increase [1]. Simulations are performed, with the multi-carrier Peleg-trellis inner-decoder, to determine the MSDD coding gain for different values of S_m. The simulation results will be discussed in Section V.

B. Joint and iterative multi-carrier trellis-based MSDD and BCJR decoding

As explained in Section III-E; the BCJR outer-decoder yields estimates $\left\{\hat{b}_i\right\}$ of the information bits and extrinsic probabilities $\left\{\tilde{P}\left(x_t^i\right)\right\}$ of the coded bits.

The "extrinsic" probability pair $\left(\tilde{P}\left(x_t^1\right), \tilde{P}\left(x_t^2\right)\right)$ is fed back to the inner-decoder as the a-priori information $\Pr\{\Delta\phi_t\}$ of QPSK symbol $\hat{q}_t$ and the branch probability given by (29) can be rewritten as:

$$\gamma_t(\eta_m) = \begin{cases} \Pr\{\Delta\varphi_t\}\Pr\{r_t\,|\psi_t\}, & t = nL_m \\ \left[\tilde{P}\left(x_t^1\right)\tilde{P}\left(x_t^2\right)\right]\Pr\{r_t\,|\psi_t\}. & t \neq nL_m \end{cases} \tag{34}$$

Simulations are performed to determine the MSDD iterative coding gain of joint and iterative S_m-length MSDD and SiSo convolutional decoding for DE-COFDM systems. The S_m-length MSDD is performed with the multi-carrier Peleg-trellis inner-decoder and the convolutional decoding is performed with the BCJR outer-decoder. The simulations results, for different values of S_m and for a different number of iterations I, will be discussed in Section V.

V. Simulation results of the systems

The simulations of the single-carrier Peleg-trellis inner-decoder, shown by Figure 2, are performed for $L_m = 2, 4, 18$ and with $I = 1, 2$ iterations, where $I = 1$ stands for no iterations and $I = 2$ is one iteration. The curves show the signal to noise ratio $E_b/N_0 = 1/\sigma_\eta^2$ versus the BER for a linear AWGN channel with a constant carrier phase and where the receiver employs matched filtering, as given by (5). The specifically chosen values for L_m are based on commonly used frame-sizes for services broadcasted by the DAB, DAB+ and T-DMB DE-COFDM broadcast systems in transmission Mode-I, where the maximum number of interleaved OFDM symbols is equal to eighteen and the curve for $L_m \approx \infty$ is a reference curve for the MSDD (iterative) coding gain. Figure 2 shows that a higher value of L_m i.e. increasing the length of the Peleg-trellis increases the MSDD coding gain and the largest MSDD coding gain is obtained for the maximum number of interleaved OFDM symbols of eighteen, this is also achieved in the iterative case as can be seen from Figure 2 for $I = 2$.

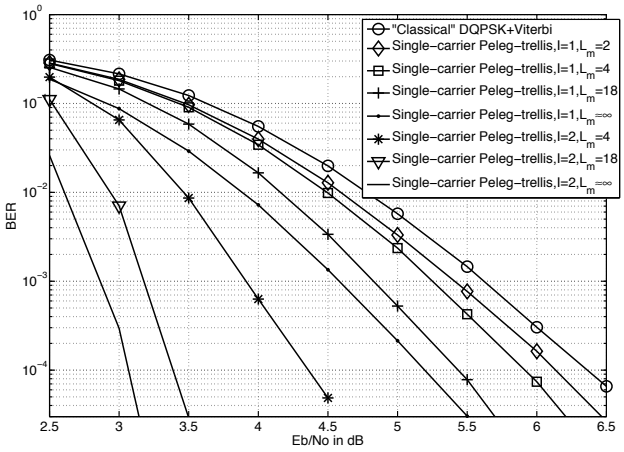

Fig. 2. BER Single-carrier Peleg-trellis inner-decoder.

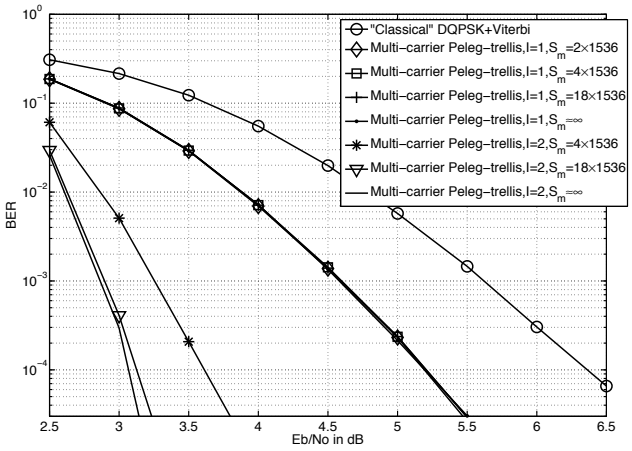

Fig. 3. BER Multi-carrier Peleg-trellis inner-decoder.

The simulations of the multi-carrier Peleg-trellis inner-decoder, shown by Figure 3, are performed for $S_m = (2, 4, 18) \times 1536$ with $I = 1, 2$ iterations. The specifically chosen values for S_m are based on transmissions in Mode-I, where the number of OFDM-subcarriers $K_m = 1536$ and the curve for $S_m \approx \infty$ is a reference curve for the MSDD (iterative) coding gain. Figure 3 shows that the MSDD coding gain is maintained for different values of S_m where the number of OFDM-symbols are small i.e. $L_m \leq 4$, this is also achieved in the iterative case as can be seen from Figure 3 for $I = 2$.

The comparison between the single-carrier and multi-carrier Peleg-trellis inner-decoder is shown by Figure 4 and Figure 5 for transmission Mode-I with four, ten and eighteen OFDM symbols at a BER of $1 \cdot 10^{-4}$ for the AWGN channel. From Figures 4 and 5 can be seen that the multi-carrier Peleg-trellis decoder with per service symbol processing outperforms the "classical" DQPSK detection and Viterbi-decoding with soft-decisions by 1.2 dB without iterative decoding and by 2.8 dB with only one iteration iterative decoding.

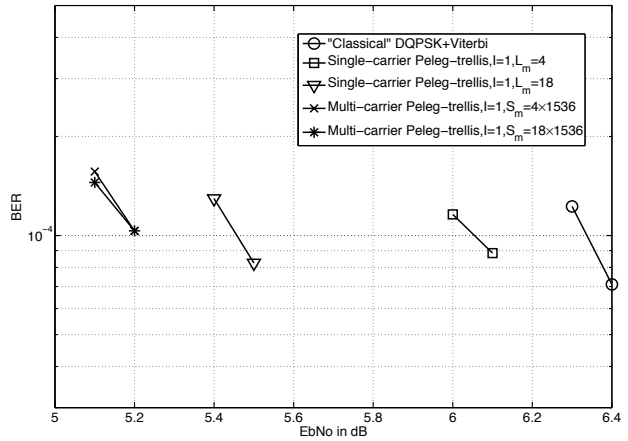

Fig. 4. BER Single- and multi-carrier Peleg-trellis decoder (non-iterative).

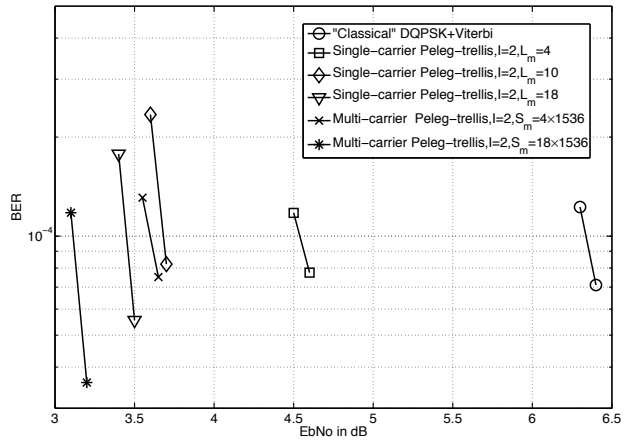

Fig. 5. BER Single- and multi-carrier Peleg-trellis decoder (one iteration).

Figures 4 and 5 also show that, with comparable receiver-complexity i.e. four OFDM symbol processing, the multi-carrier Peleg-trellis inner-decoder outperforms the single-carrier Peleg-trellis by approximately 0.9 dB.

On the other hand, comparison between the curves with $L_m = 18$ and $S_m = 4 \times 1536$ of Figure 5 reveal that the $L_m = 18$ curve shows a slightly better performance than the $S_m = 4 \times 1536$ curve. This is due to the fact that after each sequence of $(L_m - 1)$ information phases one differential phase is generated, as already stated, the differential phases can not be used in the iterative decoding process. These differential "dummy" phases will cut the trellis for the iterative decoding process i.e. *trellis-cutting* and, consequently, the MSDD iterative coding gain is slightly decreased for the $S_m = 4 \times 1536$ curve where $(L_m - 1)$ is three compared to $L_m = 18$ curve where $(L_m - 1)$ equals seventeen.

Finally, from Figures 4 and 5 can be seen that for the single-carrier Peleg-trellis inner-decoder to obtain almost similar MSDD coding gain and MSDD iterative coding gain as the four OFDM-symbol processing of the multi-carrier Peleg-trellis inner-decoder, it requires eighteen ($\approx 78\%$ overhead), respectively ten ($\approx 60\%$ overhead) OFDM-symbols to be processed. Consequently, the receiver complexity is increased up to a factor of four and a half for the single-carrier Peleg-trellis inner-decoder compared to the multi-carrier Peleg-trellis inner-decoder.

ACKNOWLEDGMENT

The authors would like to acknowledge prof.dr.ir. J.W.M. Bergmans and the management of Catena Radio Design B.V. for their support to accomplish this work.

REFERENCES

[1] D. Divsalar and M. Simon, "Multiple-symbol differential detection of MPSK," *Communications, IEEE Transactions on*, vol. 38, no. 3, pp. 300–308, Mar 1990.

[2] M. Peleg and S. Shamai, "Iterative decoding of coded and interleaved noncoherent multiple symbol detected DPSK," *Electronics Letters*, vol. 33, no. 12, pp. 1018–1020, Jun 1997.

[3] S. Benedetto, D. Divsalar, G. Montorsi, and F. Pollara, "A soft-input soft-output app module for iterative decoding of concatenated codes," *Communications Letters, IEEE*, vol. 1, no. 1, pp. 22–24, Jan 1997.

[4] S. ten Brink, J. Speidel, and R.-H. Han, "Iterative demapping for qpsk modulation," *Electronics Letters*, vol. 34, no. 15, pp. 1459–1460, Jul 1998.

[5] M. Peleg, S. Shamai, and S. Galan, "Iterative decoding for coded noncoherent MPSK communications over phase-noisy AWGN channel," *Communications, IEE Proceedings-*, vol. 147, no. 2, pp. 87–95, Apr 2000.

[6] L. Bahl, J. Cocke, F. Jelinek, and J. Raviv, "Optimal decoding of linear codes for minimizing symbol error rate (corresp.)," *Information Theory, IEEE Transactions on*, vol. 20, no. 2, pp. 284–287, Mar 1974.

[7] European Standard (Telecommunications series), "Radio broadcasting systems; digital audio broadcasting (DAB) to mobile, portable and fixed receivers," ETSI EN 300 401 V1.4.1 (2006-06), June 2006, v1.4.1.

[8] G. Zimmermann, M. Rosenberger, and S. Dostert, "Theoretical bit error rate for uncoded and coded data transmission in digital audio broadcasting," *Communications, 1996. ICC 96, Conference Record, Converging Technologies for Tomorrow's Applications. 1996 IEEE International Conference on*, vol. 1, pp. 297–301 vol.1, Jun 1996.

[9] J. Hagenauer, N. Seshadri, and C.-E. Sundberg, "The performance of rate-compatible punctured convolutional codes for digital mobile radio," *Communications, IEEE Transactions on*, vol. 38, no. 7, pp. 966–980, Jul 1990.

[10] D. Divsalar, M. Simon, and M. Shahshahani, "The performance of trellis-coded mdpsk with multiple symbol detection," *Communications, IEEE Transactions on*, vol. 38, no. 9, pp. 1391–1403, Sep 1990.